elsyca
electrochemical intelligence

176 Millard Farmer Ind. Blvd.
Newnan (Nr. Atlanta)
GA 30263
USA

Tel: +1 770 328 1346
www.elsyca.com
alan.rose@elsyca.com

Characterisation of a Zn / Ni plating bath

Report composed by Paulo Vieira, Project Engineer, Bart Van den Bossche, Engineering Manager and Alan Rose, Business Manager North American Operations

Report Documentation Page

Form Approved
OMB No. 0704-0188

1. REPORT DATE **03 SEP 2009**	2. REPORT TYPE	3. DATES COVERED **00-00-2009 to 00-00-2009**

4. TITLE AND SUBTITLE	5a. CONTRACT NUMBER
Characterisation of a Zn / Ni plating bath	5b. GRANT NUMBER
	5c. PROGRAM ELEMENT NUMBER
6. AUTHOR(S)	5d. PROJECT NUMBER
	5e. TASK NUMBER
	5f. WORK UNIT NUMBER

7. PERFORMING ORGANIZATION NAME(S) AND ADDRESS(ES) **Elsyca,176 Millard Farmer Ind. Blvd.,Newnan (Nr. Atlanta),GA,30263**	8. PERFORMING ORGANIZATION REPORT NUMBER
9. SPONSORING/MONITORING AGENCY NAME(S) AND ADDRESS(ES)	10. SPONSOR/MONITOR'S ACRONYM(S)
	11. SPONSOR/MONITOR'S REPORT NUMBER(S)

12. DISTRIBUTION/AVAILABILITY STATEMENT
Approved for public release; distribution unlimited

13. SUPPLEMENTARY NOTES
ASETSDefense 2009: Sustainable Surface Engineering for Aerospace and Defense Workshop, August 31 - September 3, 2009, Westminster, CO. Sponsored by SERDP/ESTCP.

14. ABSTRACT

15. SUBJECT TERMS

16. SECURITY CLASSIFICATION OF:			17. LIMITATION OF ABSTRACT	18. NUMBER OF PAGES	19a. NAME OF RESPONSIBLE PERSON
a. REPORT **unclassified**	b. ABSTRACT **unclassified**	c. THIS PAGE **unclassified**	**Same as Report (SAR)**	**20**	

Standard Form 298 (Rev. 8-98)
Prescribed by ANSI Std Z39-18

Table of content

1   Introduction

1.1   Cadmium replacement

For decades a suitable replacement for cadmium has been discussed and debate on the best alternative is still ongoing. Due to the toxic nature of most cadmium salts, a growing environmental pressure to reduce cadmium usage has lead some countries to ban the use of cadmium and research for alternatives was intensified. Cadmium is used for several applications due to its lubrication/friction properties in combination with corrosion protection. The lubrication ability of cadmium is an important factor in the fasteners industry, providing a corrosion protection that doesn't disturb the thread profile along with break-away torques that allow for fasteners to be mated several times without damage[1].

An additional difficulty for the replacement of cadmium is the extensive data collected over the years on cadmium's mechanical and corrosion protection properties on which industries all over the world rely on to develop new products.

A wide range of possibilities has been suggested, from electroplated and electroless deposits to physical vapour coatings. Among the candidates to replace cadmium are the zinc-nickel alloys which can outperform cadmium in corrosion tests, exhibiting a resistance in salt spray test (ASTM B 117) up to 3000 hours[2].

1.2   Zn / Ni corrosion

The Zn / Ni corrosion mechanism has been a target of investigation at least since the 90's and despite the commitment of several authors some aspects of Zn/Ni corrosion mechanism are still under debate. The initial studies aimed to find a correlation between corrosion protection and nickel content, with several studies reporting slightly different nickel content as the best protective layer.

Year	Author	% Ni
1990	Vlad, C.M. [3]	10 – 16%
1991	Pushpavanam, M. [4]	18%
1994	Alfantazi, A.M. [5]	14 – 20%
1997	H. Park [6]	13 – 15%
1999	Benballa, M.[7]	13%
2003	Sohi, M.H.[8]	13%

Table 1 – Examples of suggested Ni weight content for best corrosion protection

Higher nickel contents lead to additional problems such as limited ductility (above 20% Ni) or increasing difficulties to passivate the deposits, which is impossible in alloys containing over 25% Ni[4].

Deeper investigations introduced the importance of the phase distribution in the Zn / Ni layer, claiming that corrosion resistance was defined by the type of phase structures present in the deposit, rather than the nickel content alone. Depending on the source different phase structures have been described for the same nickel content leading to an unclear relationship between phase structure and corrosion resistance.

Source	% Ni										
	5	6	7	8	9	10	11	12	13	14	15
Thermodynamic Equilibrium[9]	$\eta + \delta$					δ	$\delta + \gamma$			γ	
Bruet-Hotellaz *et al.*[9]	$\eta_d + \gamma_d$									γ	
Lambert *et al.*[10]	$\eta + \gamma$					γ					
Wilcox *et al.*[11]						γ					
H. Park *et al.*[6]									η	$\eta+\gamma$	γ

Table 2 – Examples of reported phase structures as function of nickel content

In 1999 Bruet-Hotellaz and co-workers[9] shed some light on the phase structure debate by concluding that Zn / Ni deposits were not electrodeposited in thermodynamic equilibrium, opening the path for the idea where different process conditions can lead to different phase structures although with the same nickel content.

It has also been reported that above 15 % Ni a dezincification process occurs, leading to an alloy more noble then the steel substrate, resulting in the loss of sacrificial properties.[12]

$$\gamma \ (Ni_5Zn_{21}) \rightarrow \beta \ (NiZn) \rightarrow \alpha \ (Ni)$$
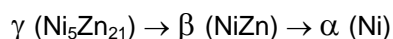
Corrosion of the Zn/Ni layer does not occur uniformly or at a steady rate, instead it occurs by a network of cracks with an accelerated corrosion in the first stages which is then slowed down by its own product of corrosion, $Zn(OH)_2$[12]. Zinc hydroxide dehydrates in time to form ZnO, however the presence of nickel in the deposit slows down the dehydration process, supporting the idea that $Zn(OH)_2$ provides a barrier on the affected areas, prolonging the corrosion protection. Zinc oxide has a higher electronic conductivity and for this reason does not slow down the corrosion rate as effectively as its hydroxide[11].
This network of crack visible in the Zn/Ni corroded surface is probably due to internal stress caused by in situ hydrogen insertion during the electrodeposition process. This is an important difference towards cadmium corrosion mechanism, which happens slowly and uniformly[12].

1.3 Polarization data

The Rotating Disc Electrode (RDE) is the most popular laboratory electrode due to its simple geometry and electrochemical capabilities, yet to plate circular coupons a Modified Rotating Disk Electrode (MRDE) was used. It consists basically a rotating working electrode in a thermostatically monitored electrolyte (double walled glass cell with water cooling / heating circuit), a reference electrode (RE) and a platinum mesh as a counter-electrode (Figure 1, Figure 2 and Figure 3).

Figure 1 – MRDE device with plastic holder (left), coupon (centre) and core rod (right)

The working electrode consists of a steel circular coupon fixed between a steel holder and a plastic cap, resulting in plastic cylinder with a steel disk at the bottom centre. The working electrode is placed on the electrochemical cell on 45 degree angle to avoid gas blockage of the surface and the Linear Sweep Voltammetry (LSV) is performed using an Autolab PGSTAT30 potentiostat.
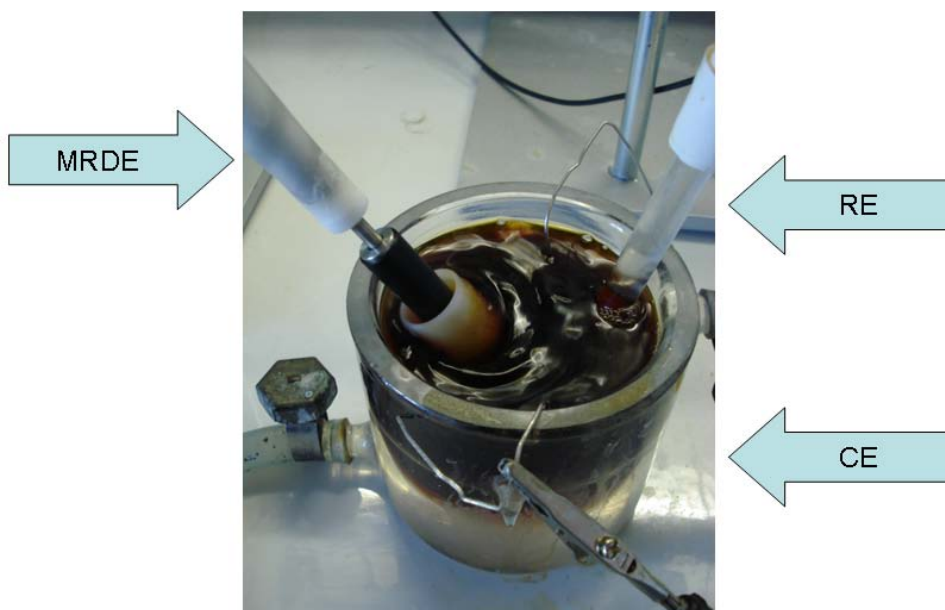

Figure 2 – MRDE laboratory set-up

The reference electrode is connected to the solution by means of a KCl salt bridge, in order to prevent contamination.

Cathodic polarisation data are obtained from Linear Sweep Voltammetry (LSV) experiments on the MRDE with a steel working electrode (*6 mm* diameter), starting from the OCP (Open Circuit Potential) up to a current density that is significantly higher than the industrially applied current density (aprox. 0 to - 500 A/m^2).

chronovoltammetric experiment   chronoamperometric experiment
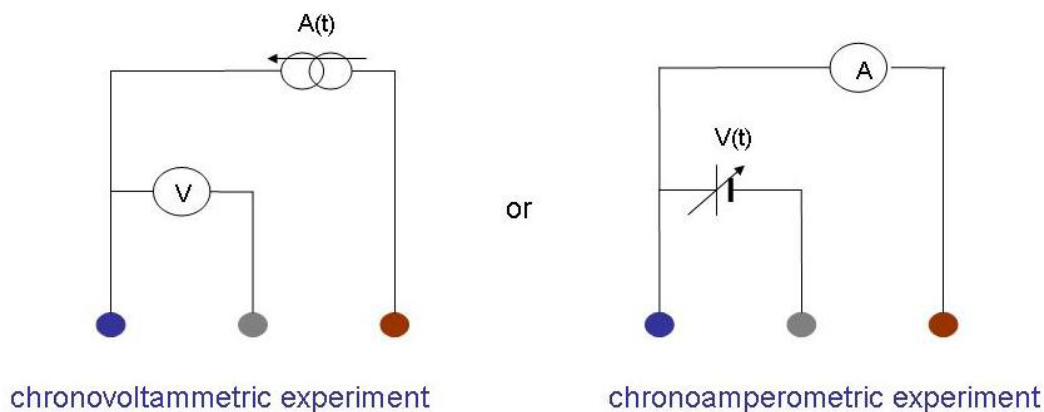
- working electrode WE for system metal / electrolyte to be investigated
- large area counter electrode CE for delivering current to the cell
- reference electrode as base for relative potential of WE (Ag/AgCl, calomel, ...)

Figure 3 – Electric configurations for performing RDE experiments

The collected polarization data is still in a raw format and must be corrected for the ohmic potential drop around the MRDE (Eq. 1)

$$\eta = E - R \, j \, A$$ **Eq. 1**

with: η electrode overpotential vs Ag/AgCl$_{sat}$ reference electrode (*V*);
  E electrode potential vs Ag/AgCl$_{sat}$ reference electrode (*V*);
  R ohmic electrolyte resistance around the RDE electrode (Ω);
  A active surface of the disc electrode (*m^2*);
  j cathodic current density on the RDE (*A/m^2*).

The ohmic electrolyte resistance R is obtained in very good approximation from an analytical expression (Eq. 2):

$$R = \frac{1}{4 \sigma r}$$ **Eq. 2**

with: r electrode radius (*m*);
  σ electrolyte conductivity (*S/m*).

LSV type polarization curves are a common tool to help understanding an electrochemical process by representing the current density in function of the applied electrode potential for a given electrolyte. While changing the potential between WE and RE linearly in time, the current response of the electrolyte is recorded

A typical cathodic polarization curve has 3 distinctive regions, a initial rise of current density up to a plateau followed by a final sharper increase.
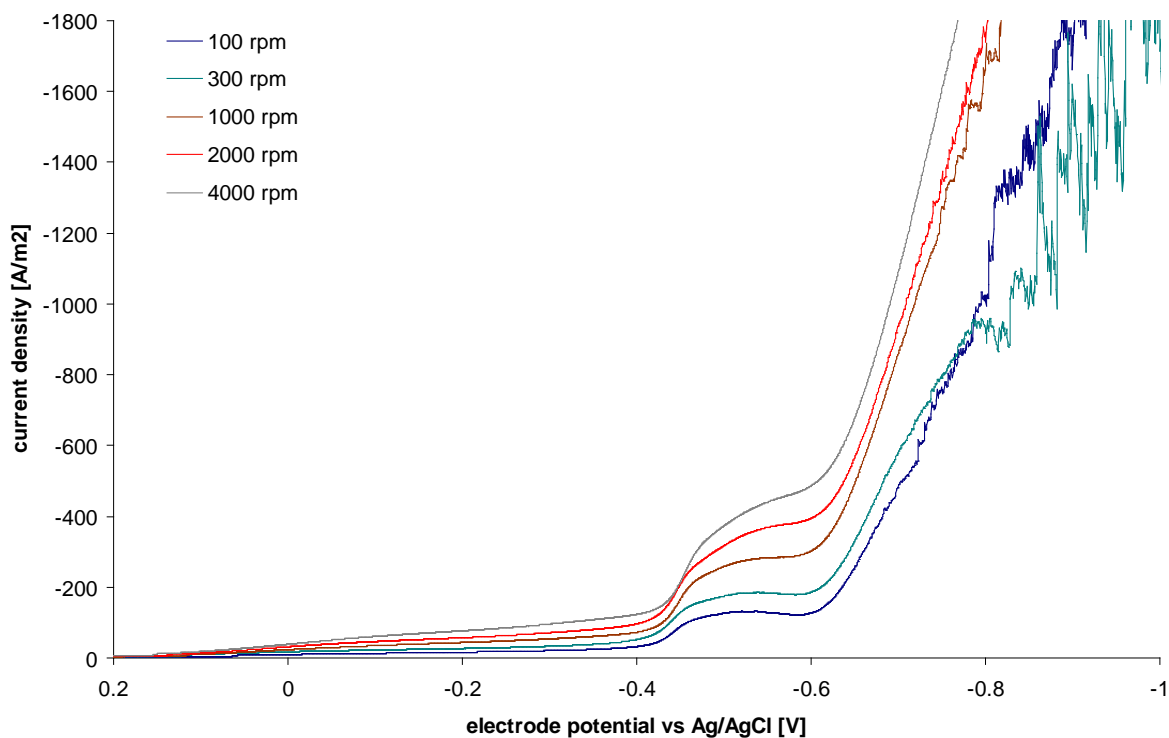

Figure 4 – Example of a platinum electrolyte polarization curve

The first rise in current density represents the initial stages of the deposition process, where the deposition rate is determined by the overpotential, this is known as the kinetic controlled region. For higher overpotential values the kinetic rate of deposition eventually is limited by the speed at which the metal ions are transported to the cathode / electrolyte surface. At this point, the mass transfer limitations will restrict the current to the so-called limiting current value, and a further increase (negative shift) in electrode potential will not have an impact in current density. For even more negative electrode potentials, the mass transfer controlled region is followed by hydrogen evolution (for aqueous electrolytes), resulting in a sharp increase in current density.

The theoretical expression for the mass transfer limited current density of a rotating disk electrode can be easily computed.

$$j_{\lim,RDE} = -0.62 \, z \, F \, D^{2/3} v^{-1/6} \omega^{1/2} c \, .$$ **Eq.3**

with:

	D	metal ion diffusion coefficient (m^2/s);
	ω	rotation speed (rad/s);
	v	kinematic viscosity (m^2/s);
	z	metal ion charge;
	F	Faraday's number (= $96500 \, C/mol$);
	c	metal ion bulk concentration (M/m^3);
	j	cathodic mass transfer limited current density (A/m^2).

As seen in Figure 4, equation (3) indicates that an increase in rotation speed improves the refreshment of ions at the electrode surface, resulting in a shift of the limiting current density to a higher value.

2   Experimental

The electrolyte characterization presented here is based on a commercially available cyanide free, alkaline Zn-Ni electrolyte (12 to 15% Ni). To eliminate any starting-up problems with a fresh bath, an electrolyte sample from an operating line was requested from a Zn-Ni electroplating company.

The sample was subjected to a carbonate removal process by lowering the electrolyte's temperature below carbonates freezing point. This process drags-out one of the additives which was replenished back to the operational concentration window prior to this experimental step.

2.1   Recommended operational parameters

The operational parameters as recommended by the supplier (excluding additives) are shown in the Table 3.

Current density	100 to 300 A/m^2 (rack) 10 to 150 A/m^2 (barrel)
[Zn]	9.0 to 11.0 g/l
[Ni]	2.0 to 2.8 g/l
Temperature	26°C
Anodes	Pure nickel anodes

Table 3 – Operational parameters recommended by the electrolyte supplier

For the bath sample examined within the scope of this project, the Ni content was at the lower limit of the recommended operational window (i.e. 2.0 g/l).

2.2   Cathodic polarization

Cathodic polarization data were recorded as described in Section 1 for 3 different hydrodynamic conditions. Hydrodynamic conditions around rotating electrodes are well known and can be adjusted by setting the rotation speed of the electrode. For the present work, the selected rotation speeds were:

a)   100 RPM – equivalent to natural convection

b)   400 RPM – low forced flow

c)   1200 RPM – high forced flow (but still laminar)

Carbon steel coupons were degreased in acetone and then freed from oxides in a chemical pickling solution of hydrochloric acid (10% volume) for 10 to 15 minutes.

The conductivity of the electrolyte at 26°C was recorded as 11.5 S/m at a pH value of 13.8.

The polarization curves at these 3 different rotation speeds are presented in Figure 5.
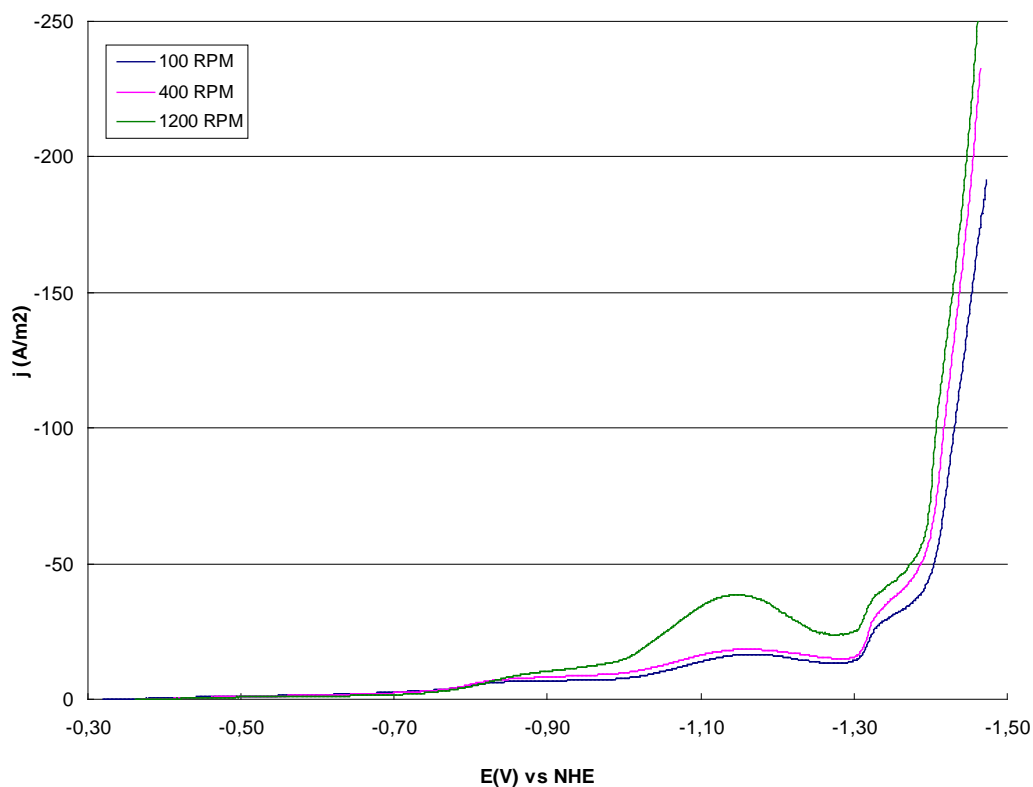
Figure 5 – Polarization curves for 3 different rotation speeds

The curves each show 2 plateaus, the first being Ni deposition limiting current which is consistent with dark nickel rich areas found at very low current densities. A limiting current plateau is observed, but the increasing slope of this plateau suggests that kinetically controlled Zn deposition is already taking place.   At higher current densities the Zn deposition limiting current occurs, being followed by a passivation region (preventing a limiting current plateau from occurring).   The passivation behaviour disappears for even more negative electrode potential values due to the initiation of hydrogen evolution.

At 200 A/m^2, being the operational current density that is recommended by the supplier for rack applications, the process is situated in the hydrogen evolution region, implicating that both metals are

deposited under mass transfer limiting conditions. This enhances the importance of both electrolyte refreshment (flow) and control of the metal concentration in the electrolyte for obtaining a relatively constant alloy composition up to very high current densities.

At low current densities, one or both metals might be deposited under kinetic control, and in that case the ratio of plated metals will not be constant.

Below 15 A/m^2 (natural convection and moderate forced flow) zinc is not yet in mass transfer limitation and therefore its ratio in the alloy will gradually decrease as current density decreases.

Conductivity has an important impact on the throwing power of the electrolyte. The value as recorded here (11.5 S/m) is at the lower end of industrial aqueous plating baths, hence indicating poor throwing power.

Also the slope of the polarisation curve determines the throwing power of the electrolyte. For this Zn / Ni electrolyte the entire current density operation window (100 to 300 A/ m^2) is within a 60 mV potential range. This again indicates a low throwing power of the electrolyte.

2.3 Cathodic efficiency

Cathodic efficiency represents the ratio between the current that is used in the plating process and the current used in hydrogen gas evolution. The electrolyte supplier claims a cathodic efficiency between 50 and 60%, since no reference is made to what current density interval, it is assumed that this efficiency is related to 100 to 300 A/m^2.
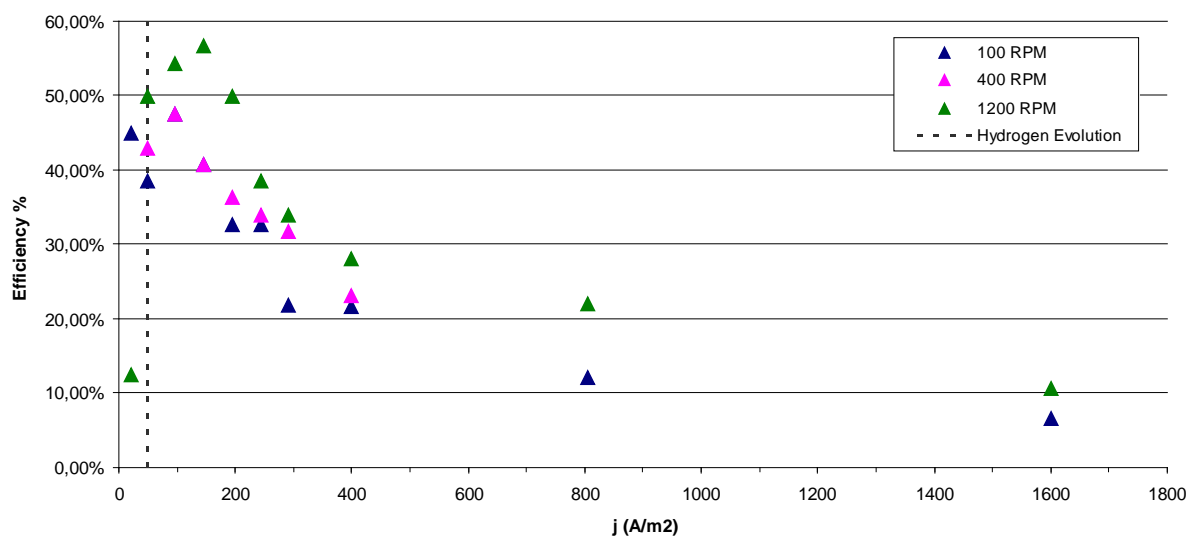
Figure 6 – Efficiency as a function of current density for 3 different rotation speeds

This announced efficiency is indeed obtained within the recommended current density interval [100, 300 A/m^2] although only for higher agitation regimes (figure 6). For natural convection and mild forced flow conditions efficiency values are somewhat smaller and the maximum efficiency is shifted towards lower current densities (100 A/m^2).

At very lower current densities the process shows a lower plating efficiency because some of the electrical charge will be lost to either partial reduction of the metals or to reactions with other species present in the electrolyte.

As current densities increase, the efficiency sharply rises to it maximum value. Around 50 A/m2 hydrogen starts to evolve (see figure 6) causing a deceleration in plating efficiency rise, and soon hydrogen evolution becomes dominant over the plating process. At this point a maximum efficiency is observed and further increase in current density progressively boosts hydrogen evolution, resulting in significant efficiency drop.

At higher convection rates the ion refreshment at the cathode surface is more efficient causing the limiting current density for both Ni and Zn deposition to be increased. Since the initiation of hydrogen evolution is not affected by hydrodynamics, the peak efficiency value will be shifted to more negative electrode potentials.

2.4 Alloy composition

As described in section 1, it is generally agreed that above 15% weight Ni content leads to a large drop in corrosion resistance.

This Zn / Ni plating process targets an alloy composition with nickel content between 12 and 15% and even though a lot of points fall within this range, non-conformities can still be found within the operational window (Figure 7).
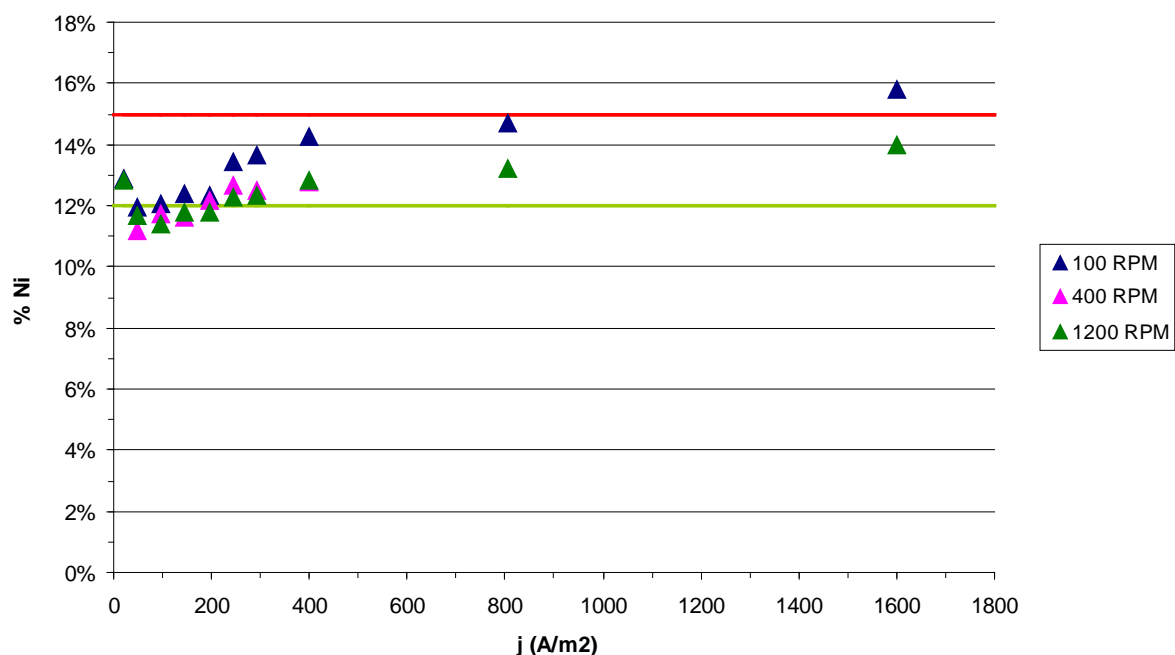
Figure 7 – Ni content in alloy composition

In fact from 100 to 300 A/m^2 most current densities result in Ni poor alloys, especially for the higher convection cases (see figure 6).

It has to be remembered that the electrolyte is operated with a nickel concentration at the lower end of the interval as recommended by the supplier. This is the main cause for the Ni content being below 12 % for low current density values. It is reasonable to assume that if the Ni concentration in the electrolyte would be increased, a slight uplift to higher Ni content in the deposit would be visible, bringing the low current density deposits above the 12 % Ni mark. On the opposite side, this correction would also cause the high current density deposits to contain more Ni. With the present Ni concentration in the electrolyte only for very high current densities the 15 % Ni threshold is reached, but for natural convection a single 1% increase in Ni content would trespass the 15% Ni limit even within the operational current density window.

It is observed that in the operational current density interval [100 - 300 A/m^2] the alloy composition is only slightly affected by the flow conditions. For higher current densities however, convection becomes increasingly important, and higher convection rates will be required to keep the Ni content in the deposit below 15 %.

At very low current densities (< 20 A/m^2) another increase in Ni content is observed, but this is easily explained by the Zn deposition reaction not yet being under mass transfer limitations.

2.5 Roughness

Although determination of the Ni content in the deposit is the main goal of this study, roughness (R_a value) was also evaluated, since roughness might have an impact on the corrosion protection of the layer, especially if the roughness is of the same order of magnitude at the total deposit thickness.

In order to restrict the plating times (mainly for the low current density samples) 2 micron thick layers were plated. For this reason a strong influence of the substrate's roughness is still observed in the measured deposit roughness values. However, it can be clearly observed from Figure 8 that a combination of poor hydrodynamics with high current densities leads to a rapid increase of the observed roughness value.
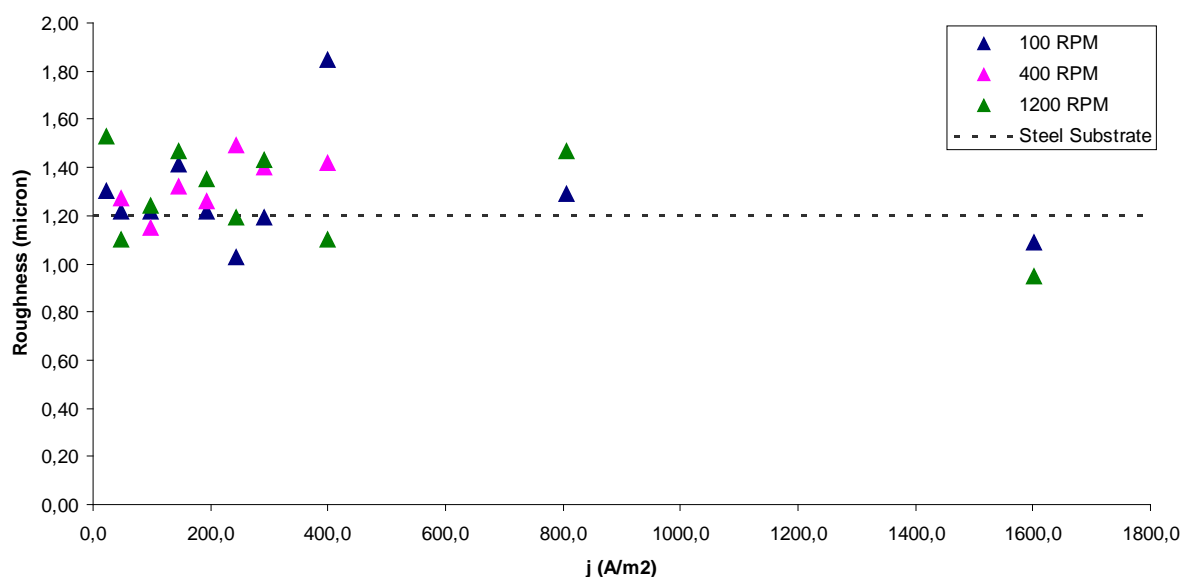
Figure 8 – Roughness as function of current density

From this set of measurements it can only be concluded that up to 2 microns the Zn-Ni layer follows the roughness of the steel substrate being used.
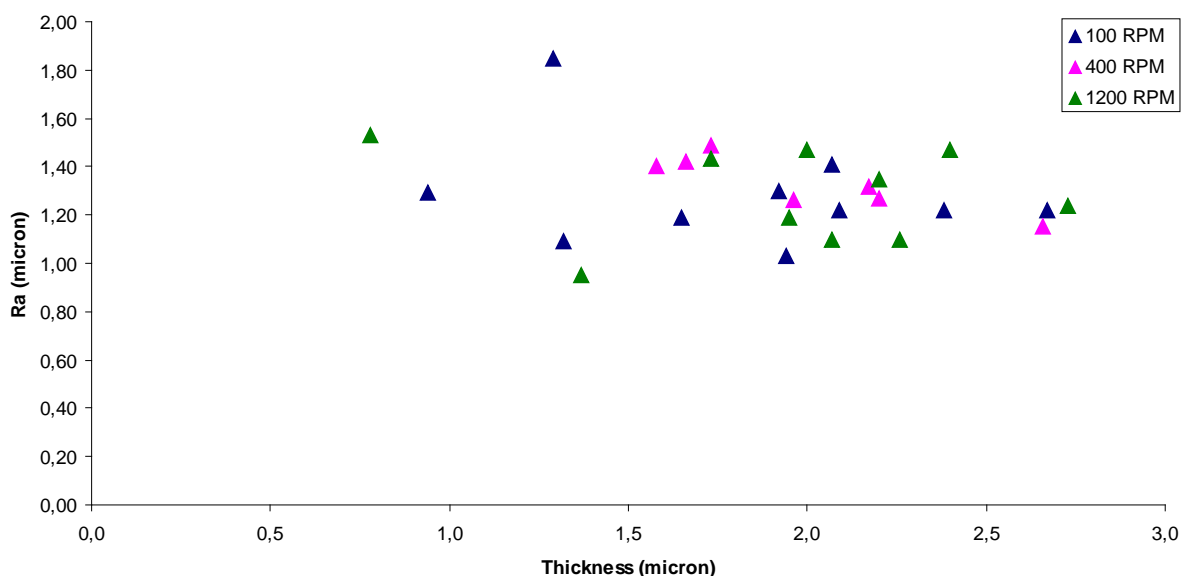
Figure 9 – Roughness as function of layer thickness values

Taking in to account the achieved thickness of the plated layer, results suggest that the roughness of the layer reduces with increasing layer thickness. However further tests with a thicker plated layer are required to reach decisive conclusions.

3　Simulations

Figures 10 to 12 show some preliminary results for respectively the Zn-NI layer thickness distribution, current density distribution and Ni content distribution over a landing gear part of considerable size and geometrical complexity. This simulation was performed using only main anodes at respectable distance from the part, for an average imposed current density of 300 A/m^2 over the surfaces to be plated. Plating time was set to 30 minutes. The deposit thickness and current density show a huge variation over the part, whereas the Ni content drops below 0.12 % weight fraction in the low current density areas.
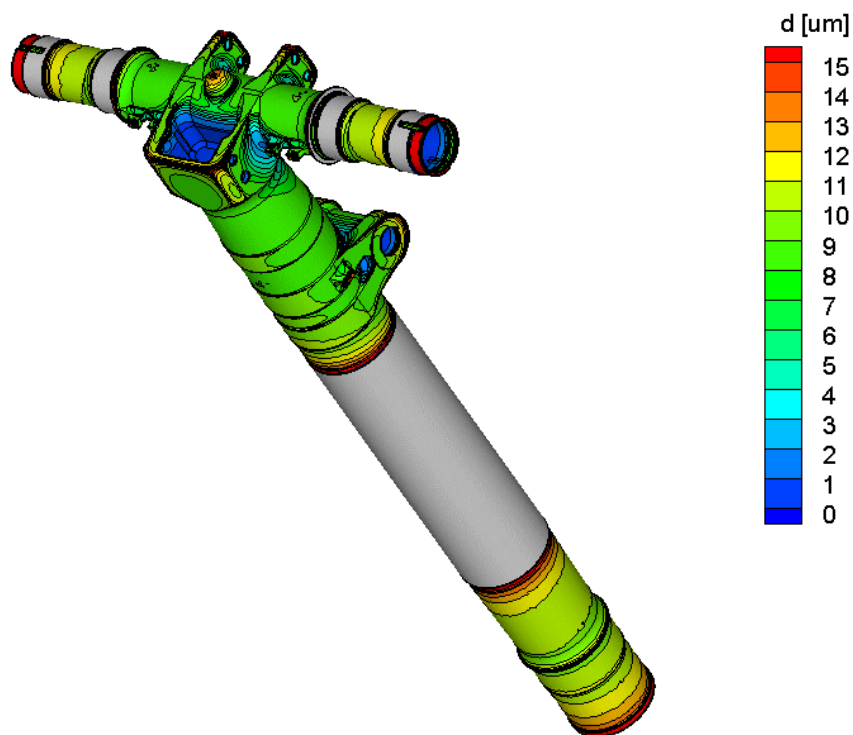
Figure 10 – simulated Zn-Ni layer thickness distribution over a landing gear part
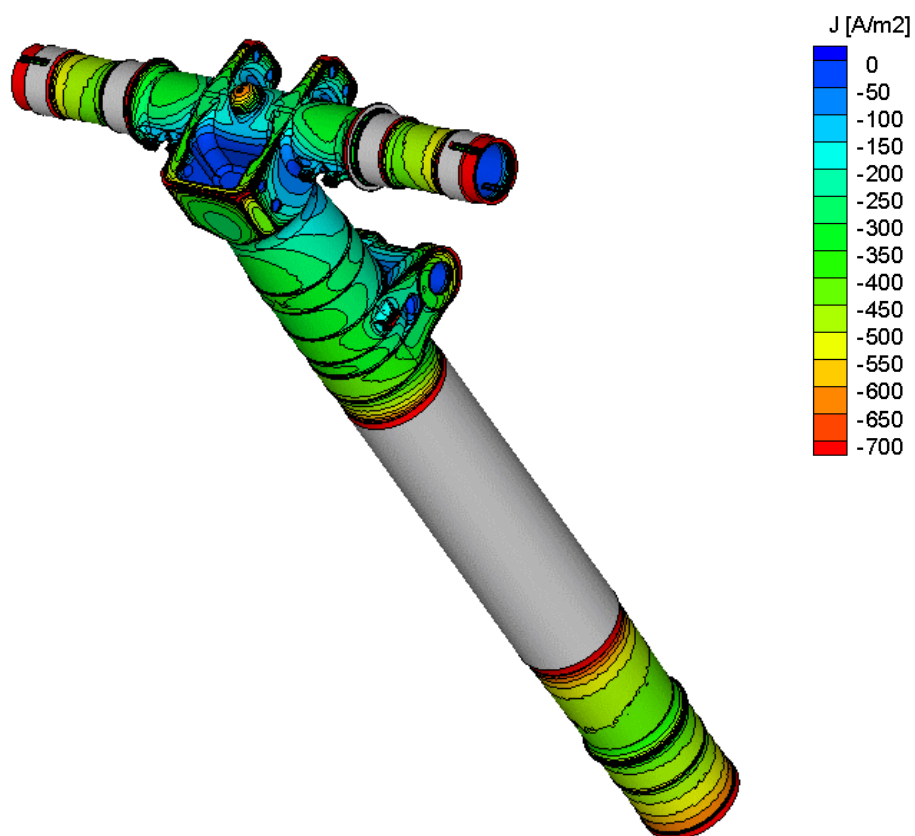
Figure 11 – simulated Zn-Ni current density distribution over a landing gear part
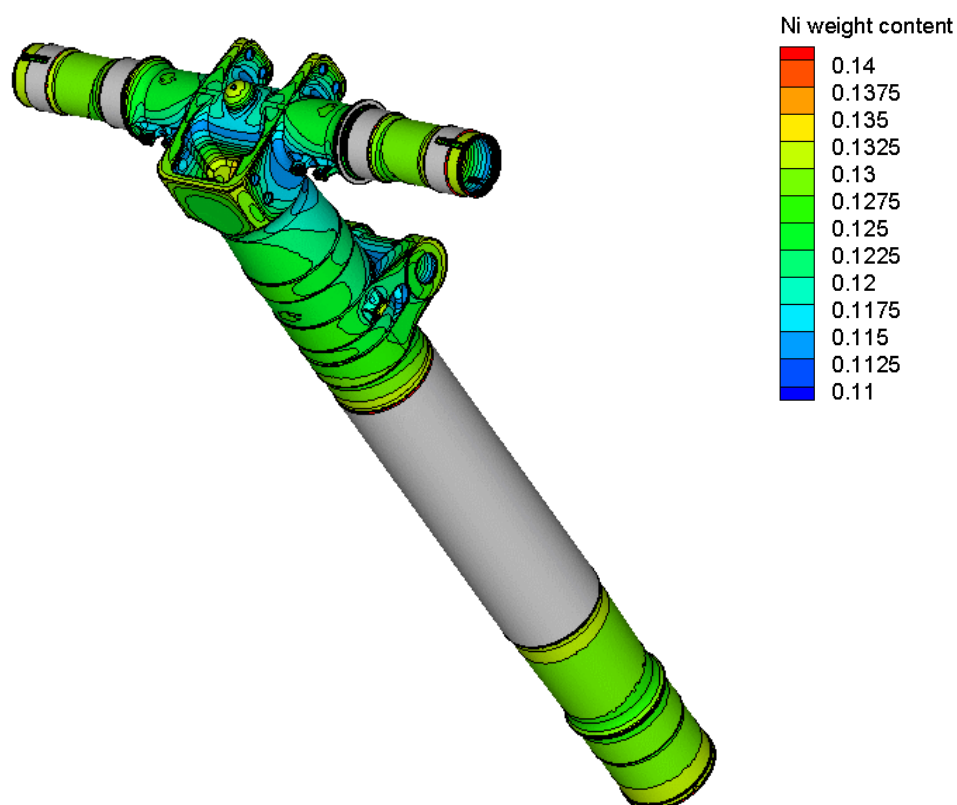
Figure 12 – simulated Ni content in the Zn-Ni deposit over a landing gear part

4   Discussion

4.1   Current density distribution

From a general point of view, the Wagner number is a measure for predicting the degree of non-uniformity in current density distribution over a surface to be plated. Hence also for this Zn-Ni electroplating processes, the Wagner number will allow to predict - to some extent - the degree of non-uniformity that can be expected.

Equation 4 shows the Wagner number definition.

$$Wa = \frac{\partial(V_c - U_c)/\partial j_c}{\rho\,L} \qquad\qquad \textbf{Eq.4}$$

The numerator of equation 4 contains the 'polarization resistance', more precisely the inverse of the slope of the polarization curve at the 'working point' (i.e. for the average cathodic current density j_c). The denominator represents the ohmic drop in the electrolyte over a field line.

The numerator is easily obtained as the inverse of the derivative of the polarization curve at the average cathodic current density j_c. For the recommended current density of 200 A/m^2, this value is about 3.8E-4 Vm^2/A at 100 RPM and about 3.2E-4 Vm^2/A for higher RPM values.

The denominator requires a proper definition of the characteristic length L. For a first approach, a suitable definition is the length between the most recessed and most protruding point of the part to be plated. When focusing on aviation landing gear parts, a typical value would be L = 0.1 m, which results in Wagner number of about 0.04.

For Wagner numbers $\gg$ 1, nearly no non-uniformity will occur (= 'secondary' current density distribution), while for Wa $\ll$ 1, severe non-uniformity in current density and deposit thickness will occur (= 'primary' current density distribution).

Hence for Zn-Ni coatings being applied to large parts with important 3D topology of the surfaces to be plated, severe problems with the non-uniformity of current density, layer thickness and deposit composition, can be expected. This suggests that dedicated conforming anode systems be used for each landing gear program, even beyond the state-of-art conforming anode systems as used for Cd plating processes.

In addition, the flow conditions (electrolyte refreshment) along the surfaces to be plated will be strongly dependent on the type and configuration of flow agitation being used in the Zn-Ni plating tank, and on the geometry, positioning and orientation of the landing gear part in the tank. Given the fact that both total plating efficiency and alloy composition depend on the local flow conditions, a dedicated forced flow system for each landing gear part programs also seems unavoidable.

The polarization resistance can be influenced by changing the electrolyte composition, in particular the additives (type and concentration). Additives such as levelers and brighteners can lower the slope of the polarization curve, especially in the region below 200 A/ m^2. But this is only possible for kinetically controlled plating processes, it will not affect a plating process that is under complete mass transfer control.

The conductivity of this Zn-Ni electrolyte is similar to the conductivity of some widely used electrolytes, such as Ni Watts and Ni sulphamate type baths. But it is worth noting that – for example - for industrial acid copper plating solutions, the conductivity is easily 5 times higher, and the additives being used commercially often lower the polarization resistance significantly. As a result, most industrial acid copper plating baths have a throwing power that by far outperforms the throwing power of Zn/Ni baths.

4.2   Electrolyte maintenance

As for most alloy plating electrolytes, the maintenance of the Zn/Ni electrolyte is critical. Different commercial electrolytes have different approaches to the configuration of the additives, often suppliers group a set of additives in one solution while some supply the components individually. In the present case a set of 5 different additives was necessary to maintain/correct the electrolyte to within the specified tolerances. In addition to organic additives, nickel concentration is also maintained by dosing a nickel concentrated solution while zinc is often replenished using metallic zinc. Unlike other electrolytes where metal pellets are used as anodes in the plating tank, in Zn / Ni electrolytes the metallic zinc dissolves by chemical dissolution in a separated tank. To maintain the zinc concentration a volume of this zinc rich electrolyte is added to the main electrolyte on an Ampere-hour base.

To properly maintain the metal ratio in the electrolyte monitoring is required at least twice a day, preferentially by X-ray fluorescence or alternatively by titration. If nickel is easy to replenish, care must be taken to ensure a constant zinc concentration in the zinc dissolution tank.

Despite each additive / metal being added continuously during production more often then desired this delicate balance is disrupted and scrap rates consequently increase dramatically. Since most companies do not possess the advanced analytical techniques to properly quantify organic additives, only an empirical approach remains to ensure a balanced electrolyte. This often relies on a number of Hull cell panels made with different additive concentrations to determine the best corrective action.

Although Zn/Ni works very well when balanced, it is not an easy electrolyte to maintain neither preventively or correctively.

5   Conclusions

It has been stated that 15 weight % in nickel content is the threshold above which corrosion resistance drops significantly and in the scope of the present study it has been seen that for a broad range of current densities and flow conditions the deposit remains below this level.

However, it has also been stated that the present electrolyte was used with a nickel concentration at the lower end of the recommended concentration window, which prevents at higher current densities trespassing the 15% limit, but results in poor nickel content at the normal range of current density values. This type of electrolyte is designed to produce an alloy with at least 12% in nickel, below which corrosion protection is also reduced.

As seen in the previous section, electrolyte maintenance is not trivial and a lack of balance in metals or additives can easily promote a shift to higher nickel contents, thereby trespassing the 15 % weight barrier.

Due to the low Wagner number values that are encountered for this electrolyte, the use of properly designed conforming anodes will be unavoidable for nearly any aerospace component being Zn/Ni plated.

The sensibility of the Ni content in the deposit towards flow conditions also urges for well controlled flow conditions.

Similar performance studies could be made for other Zn/NI baths (e.g. acidic ones) or even other candidate cadmium replacing alloy plating systems, such as Sn / Zn.
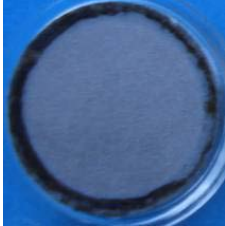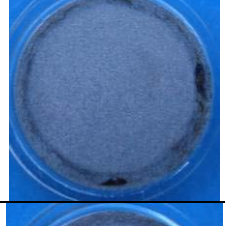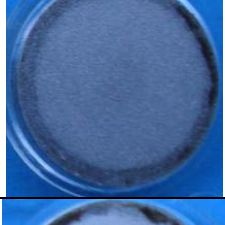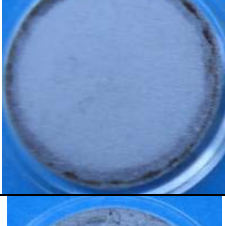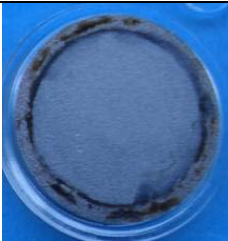
6   References

[1] – Groshart, E., Metal Finishing, 1997, **95**, 79
[2] – Brooman, E.W. Metal Finishing, 2000, **98**, 42

[3] – Vlad, C.M., Symposium on Zinc-based steel coating systems, ed. G. Krauss and D.K. Matlock, Detroit, Michigan, 7-11 Oct. 1990, p. 129

[4] – Pushpavanam, M., Natarajan, S.R., Balakrishnan, K. and Sharma, L.R., Journal of Applied Electrochemistry, 1991, **21**, 642

[5] – Alfantasi, A.M., A study on the synthesis, characterization ans properties of pulse-plated ultrafine-grained Zn-Ni alloy coating. Ph.D. thesis, Queen's University, Kingston, Ontario, 1994

[6] – Park,H. and Szpunar, J.A., Corrosion Science, 1998, **40**, 525

[7] – Benballa, M., Nils, L., Sarret, M. and Muller, C., Surface and Coating Technology, 2000, **123**, 55

[8] – Heydarzadeh Sohi, M. and Jalali, M., Journal of Materials Processing Technology, 2003, **138**, 63

[9] – Bruet-Hotellaz, Bonino, J.P. and Rousset, A., Journal of Material Science, 1999, **34**, 881

[10] – Lambert, M.R., Hart, R.G. and Townsend, H.E., SAE, 1983, n°831817, 1153

[11] – Wilcox, G.D., Gabe, D.R., Corrosion Science, 1993, **35**, 1251

[12] – Gavrila, M., Millet, J.P., Mazille, H., Marchandise, D. and Cuntz, J.M., Surface and Coating Technology, 2000, **123**, 164
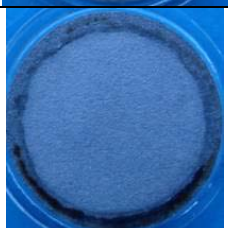
7   Annex I - Pictures
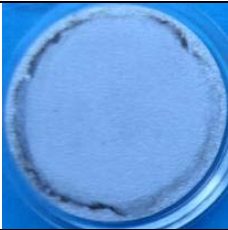
7.1   100 RPM

RPM	A/m2	Image
100	22	
100	50	
100	100	
100	150	
100	200	
100	250	
100	300	

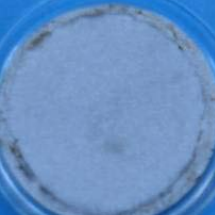| 100	400	
100	800	
100	1600	
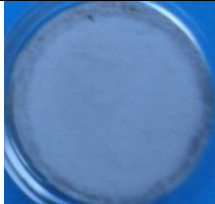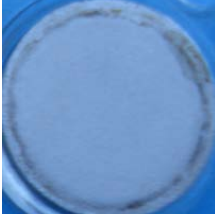
7.2 400 RPM

RPM	A/m2	Image
400	50	
400	100	
400	150	
400	200	

400	250	
400	300	
400	400	

7.3 1200 RPM

RPM	A/m2	Image
1200	22	
1200	50	
1200	100	
1200	150	

September 3, 2009

1200	200	
1200	250	
1200	300	
1200	400	
1200	800	
1200	1600	

September 3, 2009